International Journal of Advanced Engineering, Management and Science (IJAEMS)
Peer-Reviewed Journal
ISSN: 2454-1311 | Vol-11, Issue-5; Sep-Oct, 2025
Journal Home Page: https://ijaems.com/
DOI: https://dx.doi.org/10.22161/ijaems.115.1

New concept for Simulating the Cavitation Phenomenon by using Sub-grid Model for Characteristic the Fine Structures

Asya Abd Alelah Alabdalah

Department of ITE, SVU University, Syria

Received: 29 Jul 2025; Received in revised form: 25 Aug 2025; Accepted: 31 Aug 2025; Available online: 04 Sep 2025

Abstract *— Cavitation occurs in liquid flows at the operation temperature, when the local pressure reaches values lower than the vapor pressure, inducing vaporization, this phenomenon causes some potentially negative effects such as: performance deterioration, vibration noise and cavitation erosion. This research is working on the development of new approach for simulating the cavitation phenomenon by using sub-grid model for characteristic the Fine Structures which are used for simulating the cavitation phenomenon which relay on using sub-grid model to characteristic the fine structures whose are responsible for the dissipation of turbulence energy into heat as well as for the molecular mixing, these fine structure gives the space for reactions to occur*

Keywords *— **cavitation model, eddy dissipation concept, Eulerian model for Cavitation, eddy dissipation concept***

I. INTRODUCTION

Cavitation occurs in liquid flows at the operation temperature, when the local pressure reaches values lower than the vapor pressure, inducing vaporization, this phenomenon causes some potentially negative effects such as: performance deterioration, vibration noise and cavitation erosion.

Cavitation structures exhibit various shapes and behaviors such as

- Stable or pulsating sheet cavitation
- shedding vapor clouds

There are several methods of cavitation flow modeling

- Single phase flow modelling, which is easier in terms of calculation speed and mathematical model
- Multiphase flow modelling of the mixture of liquid, vapor and possibly other undissolved gases (uncompressible flow) with cavitation
- Multiphase flow modelling of the mixture of liquid and vapors, where the bubble dynamics are calculated in accordance with the Rayleigh – Plesset equation. This method, however, is linked with the problem of determining the number of bubbles, or cavitation nuclei.

The continuum model solves Navier-Stokes (NS) equations for the fluid mixture in an Eulerian frame is quite popular for Eulerian frame with lower gas volume fractions and weak bubble oscillations, which can ignore single bubble dynamics.

Cavitation bubbles are represented by the gas volume fraction or the gas mass fraction in the Eulerian grids, which is derived based on the expression of mixture pressure or density in the equations of state (EOSs).

©2025 The Author(s). Published by Infogain Publication, This work is licensed under a Creative Commons Attribution 4.0 License. http://creativecommons.org/licenses/by/4.0/

LE coupling formulation can be divided into two branches: one-way and two-way coupling. In one-way coupling, only the influence of the carrier phase (the carrier fluid in flow cavitation) on the dispersed phase (cavitation bubbles) is considered (under the assumption that the small bubbles move passively with the carrier fluid and that the dilute gas void fraction is rather small), so we can ignore the influence of the dispersed phase on the carrier phase. Two-way coupling increases the complexity of the nonlinear behavior of the system by considering how the dispersed bubbles influence the carrier fluid. In two-way coupling, the advection of the gas volume fraction and the pressure closure of the gas-liquid mixture are the two main challenges and still open questions

II. RESEARCH OBJECTIVE

Is the development of Eulerian model(EF) or Eulerian –Lagrange model (LE) which are used for simulating the cavitation phenomenon by using sub-grid model for cavitation phenomenon to characteristic the fine structures whose are responsible for the dissipation of turbulence energy into heat as well as for the molecular mixing, these fine structure gives the space for reactions to occur.

III. RESEARCH METHODOLOGY AND RESOURCES

A liquid at constant temperature could be subjected to a decreasing pressure, p, which falls below the saturated vapor pressure, p_v. The value of (p_v -p) is called the tension, D_p, and the magnitude at which rupture occurs is the tensile strength of the liquid, D_{pc}. The process of rupturing a liquid by decrease in pressure at roughly constant liquid temperature is often called cavitation).

IV. RESULTS AND DISCUSSION

4.1 The properties of bubble size distributions in breaking waves with the Hinze scale

In a seminal experiment on turbulent two-phase flows, Deane and Stokes (2002) performed optical measurements of bubble sizes from breaking waves in a wave flume these observations suggest that the formation of many of the bubbles larger than the Hinze scale is governed by fragmentation due to turbulent velocity fluctuations.

Define the Weber number associated with velocity fluctuations of magnitude un at a characteristic length scale l_n as

$$We_n = \rho_l . u_n^2 . l_n/\sigma = inertial\ forces/capillary\ forces$$

If ln is equal to the grid resolution Δ, and $u\Delta$ is the corresponding characteristic velocity fluctuation magnitude at this scale, then

$$We_\Delta = \rho_l . u_\Delta^2 . l_\Delta/\sigma$$

For Hinze scale lH which is assumed larger than the Kolmogorov scale corresponds to

$$We_n \sim 1$$

Then

$$l_n = l_H \sim \sigma/u_l^2\rho_l = \sigma/u_H^2\rho_l$$

As one considers length scales a little bit smaller than the Hinze scale but above the Kolmogorov scale, where the dominance of capillary-driven motion effects increasingly relative to the effects of the turbulent fluctuations. Such motion of like thin film retraction is typically associated with a Weber number of order 1 (as Taylor, 1959; Culick, 1960; Mirjalili and Mani, 2018)), which suggests that a thinning feature should be associated with a higher capillary-driven velocity uc dominate the turbulent velocity fluctuations un at the smallest scales which must have been captured by true DNS, then, requires a sufficiently small WeΔ. The dominance of inertial forces due to turbulent fluctuations over capillary forces (Wen> 1) results in the fragmentation of large features of the dispersed phase Consider an affordable LES with WeΔ≳1:

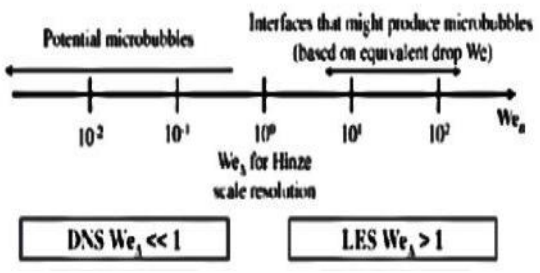

Fig.1 Schematic comparing relative length scale

If the continuous is liquid and the dispersed phase is gaseous, which yields that the microbubbles at this

©2025 The Author(s). Published by Infogain Publication, This work is licensed under a Creative Commons Attribution 4.0 License. http://creativecommons.org/licenses/by/4.0/

sizes where are closely related to the Kolmogorov scales.

Hence Kolmogorov's hypothesis of local isotropy states that at sufficiently high Reynolds numbers, the small-scale turbulent motions

$l_{0/6} \approx l_n << l_0$

are statistically isotropic and the turbulent kinetic energy is the same everywhere κ we can calculate the ratios between the Kolmogorov scale η and large scale eddies ι_o

$$l_n = l_H \sim \sigma/u_l^2 \rho_l = \sigma/u_H^2 \rho_l$$

$$l_0 \sim \kappa^{\frac{3}{2}}/\varepsilon \ , \frac{l_0}{\eta} \sim Re_{l_0}^{3/4}, Re_\eta = 1 = \frac{u_\eta . \eta}{\nu}, \varepsilon . \eta = u_\eta^3$$

Where ε the is the average rate of dissipation, and by applied Kolmogorov Scaling typically to the inertial subrange of isotropic turbulence then

$$\left[u_n^2 \sim (\varepsilon l_n)^{2/3} = (\varepsilon l_H)^{2/3} \sim (\sigma/l_H . \rho_l)\right] \rightarrow l_H \sim (\sigma/\rho_l)^{3/5} . \varepsilon^{-2/5}$$

And for large scale ιo which in Energy containing range we conclude

$$\left[l_H \sim (\sigma/\rho_l)^{3/5} . \left(\kappa^{3/2}/l_0\right)^{-2/5}\right] \rightarrow \left[\frac{l_H}{l_0} \sim \frac{\sigma^{\frac{3}{5}}}{\rho_l^{\frac{3}{5}}} . \frac{\kappa^{\frac{-3}{5}}}{l_0^{\frac{-3}{5}} . l_0}\right] \rightarrow \frac{l_H}{l_0} \sim We^{\frac{-3}{5}}$$

Then one can write

$$\left[l_H \sim l_0 . We^{\frac{-3}{5}}\right] \leftrightarrow \left[l_H \sim \eta . Re^{\frac{3}{4}} . We^{\frac{-3}{5}}\right]$$

As shown by Garrettel at. (2000) one could extend the interial subrange argument to the bubble size distribution directly, so for a bubble to be broken by the turbulent eddy its size must be equal or smaller than eddy size and at this scale weber number must be greater than 1, So the hydrodynamic pressure fluctuations $\rho_l . u_n^2$ must be larger than capillary pressure σ/r_0 . As explained by Moore & Saffman (1975) the circulation of a shear-layer eddy can be estimated to be $\Gamma = \Delta u . \lambda$, where Δu is the velocity difference a cross the share layer and λ is the distance between neighboring eddies then in simple way similar to the "Rankine vortex", considering the constant pressure inside the cavitation bubble, the pressure distributions of a cavitation vortex are as follows

$$P = P_V, \qquad (r \le r_0)$$
$$P = P_\infty - \frac{\rho \Gamma^2}{8\pi^2} . \frac{1}{r^2}, (r \ge r_0)$$

Here, P_V is assumed to be the vapor pressure at the liquid temperature, P_∞ is the pressure of the surroundings, ρ is the density, Γ is the circulation of the free vortex, and r_0 is the radius of the central core. The central core of the cavitation vortex is regarded as the cavitation bubble, the pressure at the bubble boundary $r = r_0$ can be calculated as

$$P_{bubble-boundray} = P_V = P_\infty - \frac{\rho \Gamma^2}{8\pi^2} . \frac{1}{{r_0}^2}$$

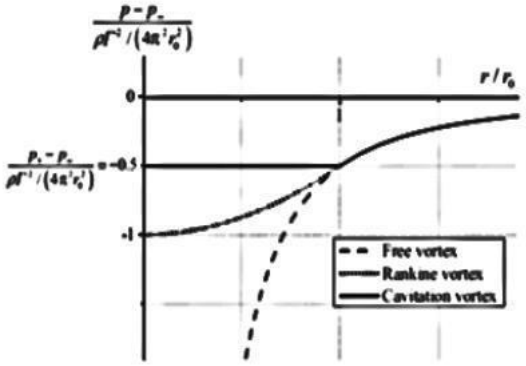

Fig. 2: shows the pressure distributions of various types of vortices

4.2 *MODELLING THE FINE STRUCTURES AND THE INTERSTRUCTURAL MIXING*

The energy spectrum characterizes the turbulent kinetic energy distribution as a function of length scale. The energy distribution at the largest length scales is generally dictated by the flow geometry and mean flow speed. In contrast, the smallest length scales are many orders of magnitude smaller than the largest scales and hence are isotropic in nature. In between, we can describe an inertial subrange bounded above by the integral scale and below by the Kolmogorov microscale

In this range, the spectrum will only be a function of the length scale and the dissipation rate, note fig.3:

©2025 The Author(s). Published by Infogain Publication, This work is licensed under a Creative Commons Attribution 4.0 License. http://creativecommons.org/licenses/by/4.0/

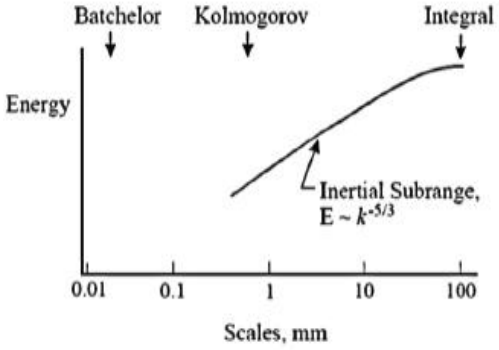

Fig.3: Typical turbulence energy spectrum, with length scales

So the first structure level is characterized by a turbulence velocity, u` , a length scale, L` , and vortices, or characteristic stain rate ω`.

The rate of dissipation $\varepsilon`$ for this level is the sum of two parts which are the first part which is directly dissipated into heat and the second one is the part of energy which transfer from the first level to the second level so,

$$\varepsilon' = \zeta^2 \left[12 \frac{u'}{l'} . u''^2 + 15 . \nu . \left(\frac{u'}{l'} \right)^2 \right]$$

the part of energy which transfer from the first level to the second level is

$$\left(\zeta^2 . 12 \frac{u'}{l'} . u''^2 \right)$$

Similarly this part of energy from the second directly dissipated into heat at the second level as

$$\left(q'' = \zeta^2 . 15 . \nu . (u''/l'')^2 \right)$$

and part of energy transfer to the third level as:

$$\left(w'' = \zeta^2 . 12 . \frac{u''}{l''} . u'''^2 \right)$$

So the model for turbulent is cleared by fig.4

This sequence of turbulence continue down to a level where all the produced mechanical energy transferred is dissipated into heat. This is the fine structure level characterized by, u*, L*, and ω*.

The mechanical energy transferred to the fine structure is

$$\left(w^* = \zeta^2 . 12 . \frac{u^*}{l^*} . u^{*2} \right)$$

and the dissipation into heat is

$$\left(q^* = \zeta^2 . 15 . \nu . (u^*/l^*)^2 \right)$$

It was shown to be in accordance with Kolmogorov's theory for its 5/3 law. We have the fine structure level characterized by, u*, L*, and ω* in inertial subring. The constant $\zeta^2 = 1$ for the energy spectrum of Kolmogorov microscale, thus for energy spectrum of the inertial subrange energy $\zeta^2 \ll 1$

by putting $\zeta = 0.18$ We have the fine structure level characterized by, u*, L*, and ω* in inertial subrang. The Re^* for this fine structure level equal to

$$\left(u^* . \frac{l^*}{\nu} = \frac{\left(\left(1.75 (\varepsilon . \nu)^{\frac{1}{4}} \right) \left(\frac{1.43 \nu^{\frac{3}{4}}}{\varepsilon^{\frac{1}{4}}} \right) \right)}{\nu} = 2.5 \right)$$

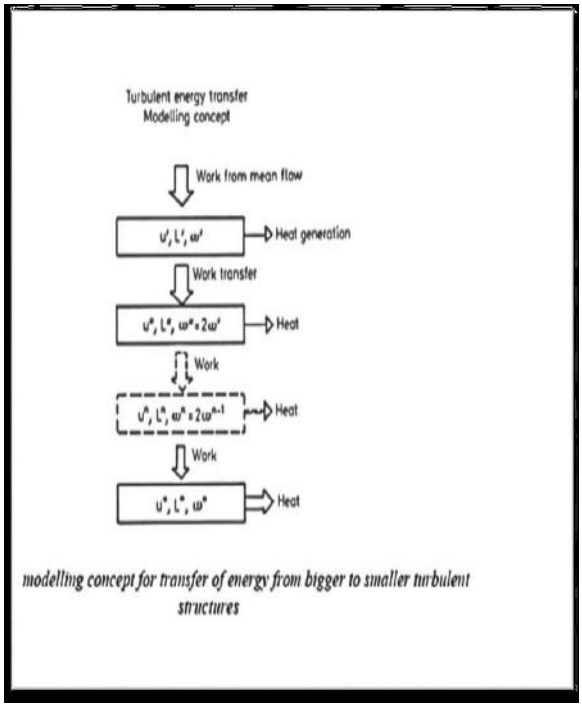

modelling concept for transfer of energy from bigger to smaller turbulent structures

Fig.4: Modeling concept for transfer of energy from bigger to smaller structure

The microscale processes concentrated in isolated regions in nearly constant energy regions where the turbulence kinetic energy can be characterized by u'2. So the mass fraction occupied by the fine structure regions can be expressed by

$$\left(\gamma^* = \left(\frac{u^*}{u'} \right)^2 \right)$$

but the fine structures whose are responsible on molecular mixing as well as dissipation of turbulence energy into heat are of the same magnitude as Kolmogorov microscales or smaller, which result in

©2025 The Author(s). Published by Infogain Publication, This work is licensed under a Creative Commons Attribution 4.0 License. http://creativecommons.org/licenses/by/4.0/

for these fine structures are very localization fashion and its linear dimensions are considerably larger than the fine structures therein, It is assumed that these structures consist typically of large thin vortex sheets, ribbons of vorticity or vortex tubes of random extension folded or tangled in the flow

The N^3 wavenumbers represented are

$$\vec{\kappa} = \kappa_0 \vec{n} = \kappa_0 \left(e_1 n_1 + e_2 n_2 + e_3 n_3 \right),$$

For integer values of n_i between $-(1/2)N+1$ and $(1/2)N$

The largest wavenumber represented is

$$\kappa_{\max} = \frac{1}{2} N \kappa_0 = \frac{\pi N}{\mathcal{L}}.$$

This spectral representation is equivalent to representing

$$\Delta x = \frac{\pi}{\kappa_{\max}} \Rightarrow \frac{\Delta x}{\eta} = \frac{\pi}{1.5} \approx 2.1.$$

The resolution of the smallest, dissipative motions, characterized by the Kolmogorov scale η, requires a sufficiently small grid spacing as clear in fig.5:

$k_{max}\,\eta \geq 1.5$

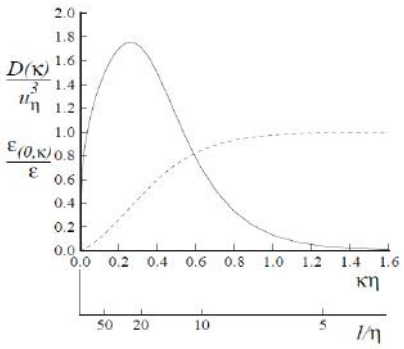

Fig.5: Dissipation spectrum (solid line) and cumulative dissipation (dashed line): $\ell = 2\pi/\kappa$ is the wavelength corresponding to wavenumber

The two spatial resolution requirements determine the necessary number of Fourier modes (or grid modes)

$$N = 2\frac{\kappa_{\max}}{\kappa_0} = 2\frac{\kappa_{\max}}{\kappa_0 L_{11}} \left(\frac{L_{11}}{L}\right)\left(\frac{L}{\eta}\right) = \frac{12}{\pi}\left(\frac{L_{11}}{L}\right)\left(\frac{L}{\eta}\right)$$

In this equation L is the scale based in the turbulent kinetic energy and the dissipation

$$L \equiv k^{3/2}/\varepsilon.$$

From experiments, it is known that

$$\left(\frac{L_{11}}{L}\right) \approx 0.43,$$

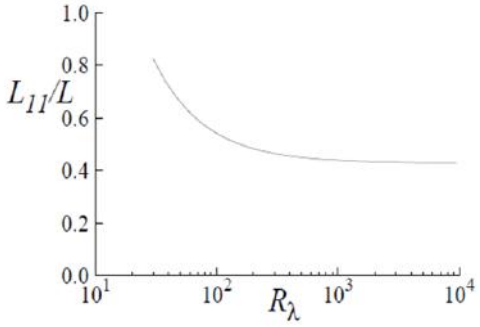

Fig .6 Show the ratio of L_{11} and L ,

The previous equation becomes,

$$\left(N = \frac{12}{\pi}(0.43)\frac{L_0}{\eta},\ \frac{\eta}{L_0} = Re_L^{-3/4}, R_\lambda = \left(\frac{20}{3}Re_L\right)^{1/2}\right) \rightarrow$$

$$\left(N = 1.6\, Re_L^{3/4} = 0.4\, Re_\lambda^{3/2} \rightarrow N^3 = 4.4\, Re_L^{9/4} = 0.06 Re_\lambda^{9/2}\right)$$

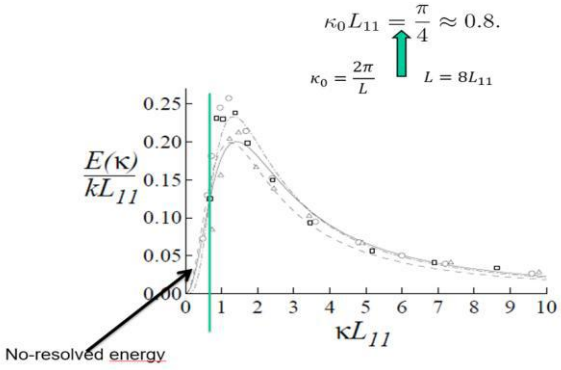

Fig.7: Show the resolved turbulent energy

For the advance of the solution in time to be accurate, it is necessary that a fluid particle move only a fraction of the grid spacing Δx in a time Δt. In practice the limit is given by the Courant-Friedrichs-Lewis (CFL) number

$$\frac{k^{1/2}\Delta t}{\Delta x} = \frac{1}{20}.$$

The duration of a simulation is tipically at least four times the turbulence time scale, $\tau = k/\varepsilon$, so the number of time steps required is

$$M = \frac{4\tau}{\Delta t} = 80\frac{L}{\Delta x} = \frac{120}{\pi}\frac{L}{\eta} \approx 9.2 R_\lambda^{3/2}.$$

©2025 The Author(s). Published by Infogain Publication, This work is licensed under a Creative Commons Attribution 4.0 License. http://creativecommons.org/licenses/by/4.0/

In result we can modify some steps in this diagram for CFD simulation:

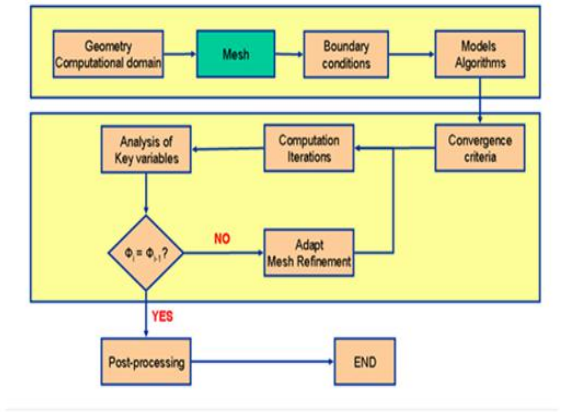

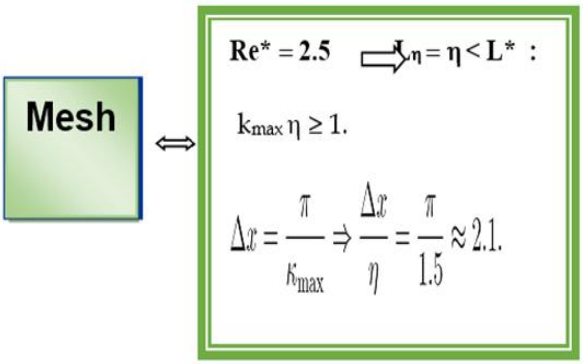

V. CONCLUSION

By modeling the molecular mixing processes in spite of modelling the turbulence chemical kinetic interaction in similar way of the applying of EDDY DISSIPTION CONCEPT the DNS frame simulation procedure will catch the features of some reactor which have cavitation phenomena within the mixing and reaction process and this is new at all for these cavitation models.

REFERENCES

[1] A.J. Coleman, J.E. Saunders, L.A. Crum, and M. Dyson. Acoustic cavitation generated by an extracorporeal shockwave lithotripter. Ultrasound in Medicine & Biology, 13(2):69–76, 1987.

[2] Y.A. Pishchalnikov, O.A. Sapozhnikov, M.R. Bailey, J.C.Williams Jr, R.O. Cleveland, T. Colonius, L.A. Crum, A.P. Evan, and J.A. McAteer. Cavitation bubble cluster activity in the breakage of kidney stones by lithotripter shockwaves. Journal of Endourology, 17(7):435–446, 2003.

[3] T Ikeda, S Yoshizawa, T Masataka, J.S. Allen, S. Takagi, N. Ohta, T. Kitamura, and Y. Matsumoto. Cloud cavitation control for lithotripsy using high intensity focused ultrasound. Ultrasound in medicine & biology, 32(9):1383–1397, 2006.

[4] C.F. Naud´e and A.T. Ellis. On the mechanism of cavitation damage by nonhemispherical cavities collapsing in contact with a solid boundary. Journal of Basic Engineering, 83(4):648–656, 1961.

[5] C.E. Brennen. Cavitation and bubble dynamics. Cambridge University Press, 2013.

[6] P.C. Etter. Underwater acoustic modeling and simulation. CRC Press, 2013.

©2025 The Author(s). Published by Infogain Publication, This work is licensed under a Creative Commons Attribution 4.0 License. http://creativecommons.org/licenses/by/4.0/